LIMITS ON $\bar{\nu}_\mu \rightarrow \bar{\nu}_e$ OSCILLATIONS FROM THE KARMEN EXPERIMENT

KLAUS EITEL

Institut für Kernphysik, Forschungszentrum Karlsruhe
Postfach 3640, 76021 Karlsruhe, Germany
E-mail: klaus@ik1.fzk.de

representing the KARMEN collaboration [1)]

ABSTRACT

The neutrino experiment KARMEN at the beam stop neutrino source ISIS investigates the oscillation channel $\bar{\nu}_\mu \rightarrow \bar{\nu}_e$ in the appearance mode by looking for $p\,(\bar{\nu}_e\,, e^+)\,n$ reactions. An analysis of data collected from February 1997 through March 2000 with the KARMEN2 experimental setup reveals 11 candidate events in good agreement with the background expectation of 12.3 ± 0.6 events. Hence, there is no indication of an oscillation signal. A maximum likelihood analysis of the data leads to an upper limit (at 90% confidence level) for the mixing angle of $\sin^2(2\Theta) < 1.3 \cdot 10^{-3}$ at large Δm^2 and $\Delta m^2 < 0.049\,\mathrm{eV}^2/\mathrm{c}^4$ for $\sin^2(2\Theta) = 1$.

1. The Experimental Configuration

The KARMEN experiment is performed at the neutron spallation facility ISIS of the Rutherford Appleton Laboratory. Neutrinos are produced by stopping 800 MeV protons in a massive beam stop target, thereby producing pions. The π^- are absorbed by the target nuclei whereas the π^+ decay at rest (DAR). Muon neutrinos ν_μ therefore emerge from the decay $\pi^+ \rightarrow \mu^+ + \nu_\mu$. The low momentum μ^+ are also stopped within the massive target and decay via $\mu^+ \rightarrow e^+ + \nu_e + \bar{\nu}_\mu$. Because of this π^+-μ^+-decay chain at rest ISIS represents a ν-source with identical intensities for ν_μ, ν_e and $\bar{\nu}_\mu$ emitted isotropically ($\Phi_\nu = 6.37 \cdot 10^{13}\,\nu/\mathrm{s}$ per flavor for a proton beam current $I_p = 200\,\mu\mathrm{A}$). There is a minor fraction of π^- decaying in flight (DIF) with the following μ^- DAR in the target station which again is suppressed by muon capture of the high Z material of the spallation target. This decay chain leads to a very small contamination of $\bar{\nu}_e/\nu_e < 6.2 \cdot 10^{-4}$ [2)], which is further reduced by software cuts.

The energy spectra of the ν's are well defined due to the DAR of both the π^+ and μ^+ (Figure 1a). The ν_μ's from π^+–decay are monoenergetic with $E(\nu_\mu)$=29.8 MeV, the continuous energy distributions of ν_e and $\bar{\nu}_\mu$ up to 52.8 MeV can be calculated using the V–A theory. Two parabolic proton pulses of 100 ns base width and a gap of 225 ns are produced with a repetition frequency of 50 Hz. The different lifetimes of pions ($\tau = 26$ ns) and muons ($\tau = 2.2\,\mu$s) allow a clear separation in time of the ν_μ-burst (Figure 1b) from the following ν_e's and $\bar{\nu}_\mu$'s (Figure 1c). The accelerator's duty cycle of 10^{-5} allows effective suppression of cosmic induced background.

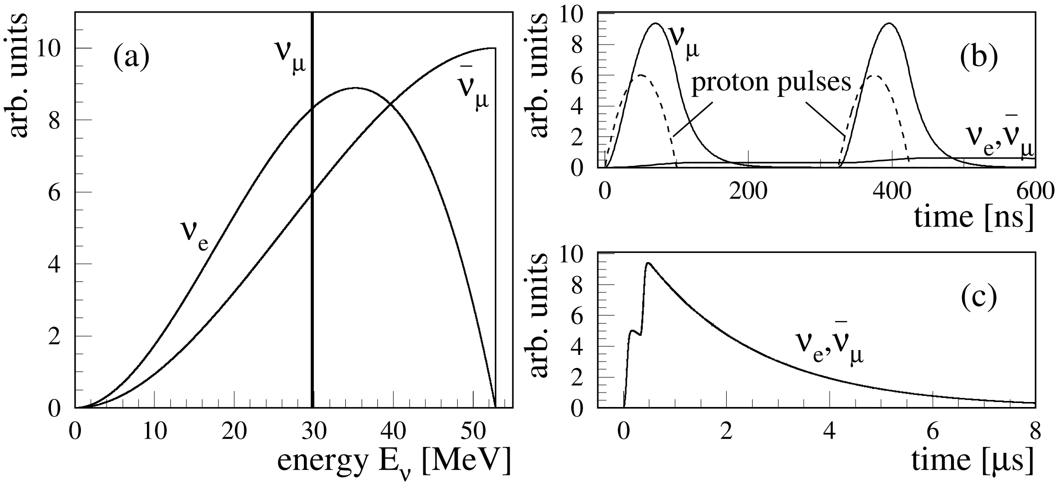

Figure 1: Neutrino energy spectra (a) and production times of ν_μ (b) and ν_e,$\bar{\nu}_\mu$ (c) at ISIS.

The neutrinos are detected in a rectangular tank filled with 56 t of a liquid scintillator [3]. The central scintillation calorimeter is segmented into 512 optically individual modules. The event position is determined by the hit module and the time difference of the PM signals at each end of this module. Gd_2O_3 coated paper within the module walls provides efficient detection of thermal neutrons due to the very high capture cross section of the Gd$\,$(n,γ) reaction ($\sigma \approx 49000\,$barn) in addition to the p$\,$(n,γ)$\,$d capture. The KARMEN electronics is synchronized to the ISIS proton pulses to an accuracy of better than $\pm 2\,$ns, so that the time structure of the neutrinos can be exploited in full detail.

A massive blockhouse of 7000 t of steel in combination with a system of two layers of active veto counters provides shielding against beam correlated spallation neutron background, suppression of the hadronic component of cosmic radiation as well as reduction of the flux of cosmic muons. In 1996 an additional third veto counter system with a total area of $300\,\mathrm{m}^2$ was installed within the 3 m thick roof and the 2–3 m thick walls of the iron shielding [4] (KARMEN2 experimental configuration). By detecting muons which pass through the steel at a distance of less than a meter from the main detector and therefore vetoing the successive energetic neutrons from muon deep inelastic scattering, the main background for the $\bar{\nu}_\mu \rightarrow \bar{\nu}_e$ oscillation search could be reduced by a factor of 40 compared to the KARMEN1 setup.

2. The $\bar{\nu}_\mu \rightarrow \bar{\nu}_e$ Oscillation Search

The signature for the detection of $\bar{\nu}_e$ is a spatially correlated delayed coincidence of positrons from p$\,$($\bar{\nu}_e$, e^+)$\,$n with energies up to $E_{e^+} = E_{\bar{\nu}_e} - Q = 52.8 - 1.8 = 51.0\,$MeV and γ emission of either of the two neutron capture processes p$\,$(n,γ)$\,$d with one γ of $E(\gamma) = 2.2\,$MeV or Gd$\,$(n,γ) with 3 γ–quanta on average and a sum energy of $\sum E(\gamma) = 8\,\text{MeV}$ (Figure 2). The positrons are expected in a time window of several μs after beam–on–target with a $2.2\,\mu$s exponential decrease due to the μ^+ decay. The time difference between the e^+ and the capture γ is given by the thermalization, diffusion and capture of neutrons, $\tau_n \approx 110\,\mu$s. The raw data investigated for this

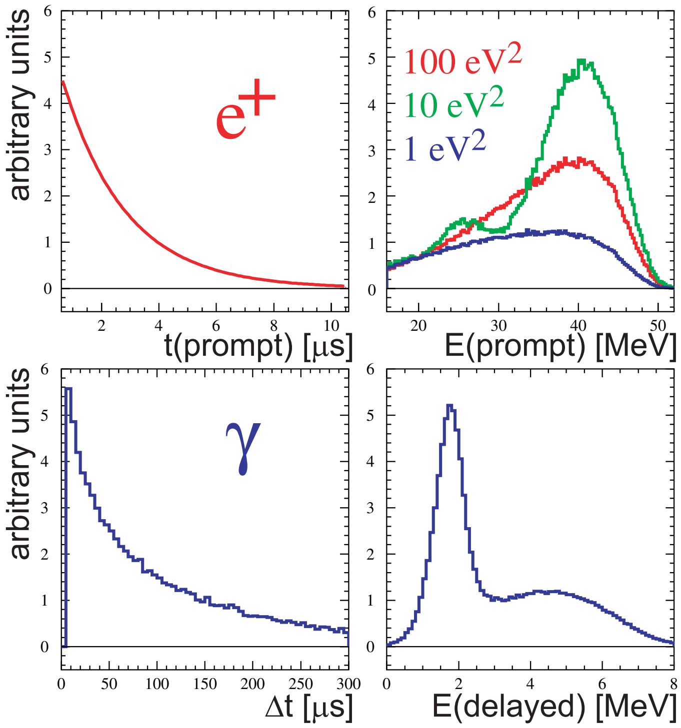

Figure 2: Expected sequences from an oscillation signal: simulated energy and time spectra of (e^+,γ) events

oscillation search were recorded in the measuring period of February 1997 through March 2000 which corresponds to 7160 C protons-on-target. A positron candidate is accepted only if there is no previous activity in the central detector nor in the two innermost veto counters up to $24\,\mu$s. The required cuts in energy and time for the prompt (p) event are: $0.6 \leq t_p \leq 10.6\,\mu$s, $16.0 \leq E_p \leq 50.0\,\text{MeV}$. The cuts on the delayed expected neutron event are as follows: $5.0 \leq t_d - t_p \leq 300\,\mu$s, $E_d \leq 8\,\text{MeV}$ and a volume of $1.3\,\text{m}^3$ for the spatial coincidence. Applying all cuts, the total background expectation amounts to 12.3 ± 0.6 sequences where the individual background sources are events induced by cosmic muons, $^{12}\text{C}\,(\,\nu_e\,,\text{e}^-\,)\,^{12}\text{N}_{\text{g.s.}}$ sequences, ν-induced accidental coincidences and (e^+,n) sequences from the intrinsic ISIS $\bar{\nu}_e$ contamination.

In Table 1 the individual contributions of the above described background sources are summarized. The last row shows the expectation of (e^+,n) sequences from oscillations assuming maximal mixing and $\Delta m^2 \geq 100\,\text{eV}^2/\text{c}^4$. The background components are determined precisely during the normal measurements: The ν induced backgrounds are measured with KARMEN in different energy and delayed time win-

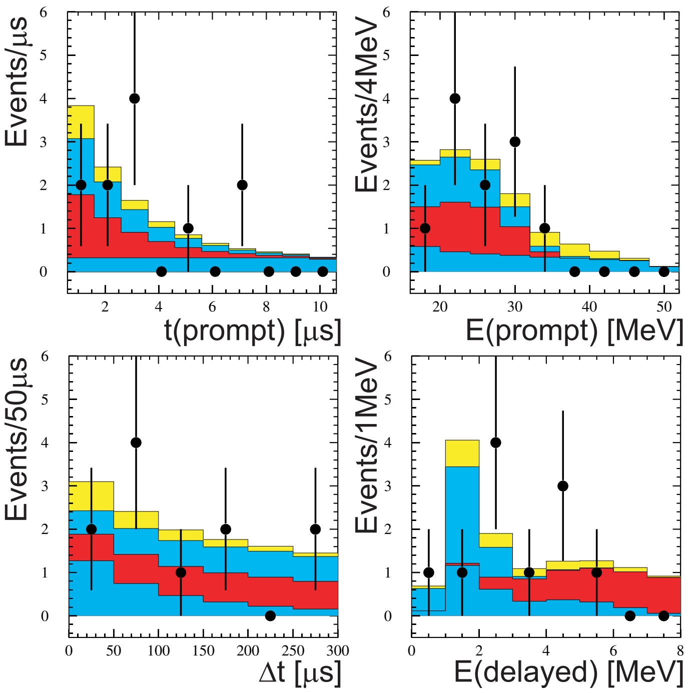

Figure 3: Spectra of the 11 candidate sequences after applying all cuts. Also shown are the background contributions (from bottom to top): cosmic background, (e^-,e^+) from ^{12}C (ν_e , e^-) ^{12}N$_{g.s.}$, ν induced random coincidences and ISIS $\bar{\nu}_e$ contamination.

Table 1: Expected sequences from different background components within the evaluation cuts specified in the text. Last row: oscillation expectation for maximal mixing.

background contribution	events
(e^-,e^+) from ^{12}C (ν_e , e^-) ^{12}N$_{g.s.}$	3.9±0.5
ν induced random coincidences	3.5±0.3
ISIS $\bar{\nu}_e$ contamination	1.7±0.2
cosmic induced sequences	3.2±0.2
total background	12.3±0.6
$\bar{\nu}_e$ signal for $\sin^2(2\Theta) = 1$	2442±269

dows, the cosmic background is measured with high statistics in the long pre-beam time window. Only the small $\bar{\nu}_e$ contribution of the intrinsic source contamination has to be simulated. In addition, the capability of the KARMEN experiment to identify neutrino induced events is constantly monitored by measuring neutrino–nucleus interactions on ^{12}C via neutral and charged current reactions.

Analysing the data results in 11 sequential events which satisfy all conditions (see Figure 3). This number is in good agreement with the total background expectation. Applying a Bayesian renormalisation of the physically allowed region to the experimental result near a boundary ($N(osc) \geq 0$, 11 measured events with 12.3 ± 0.6

background events expected), an upper limit of $N(osc) < 6.3$ at 90% CL can be extracted. An identical procedure had been applied to the initial KARMEN2 data, when the evaluation of a potential oscillation signal was based on a pure counting experiment due to the very small statistics of the background [5)].

However, with more data and spectral information, a much better evaluation method is a maximum likelihood analysis. Such a likelihood analysis to extract a possible $\bar{\nu}_\mu \rightarrow \bar{\nu}_e$ signal from these 11 sequences makes use of the precise spectral knowledge of all background sources and a detailed MC description of the oscillation signature in the detector. The likelihood function L defined as

$$L = \prod_{i=1}^{N} f(\vec{x}_i, \Delta m^2, \sin^2(2\Theta))$$

is optimised with respect to the free parameters Δm^2 and $\sin^2(2\Theta)$. The probability density function f is calculated for each of the N event sequences from the parameters $\vec{x} = (E_{prompt}, E_{delayed}, t_{prompt}, \Delta t, \Delta \vec{r})$ where Δt and $\Delta \vec{r}$ denote the delayed spatial coincidence. The analysis results in a best fit value of oscillation events $N(osc) = 0$ within the physically allowed range of parameters. As shown in Figure 4, an upper

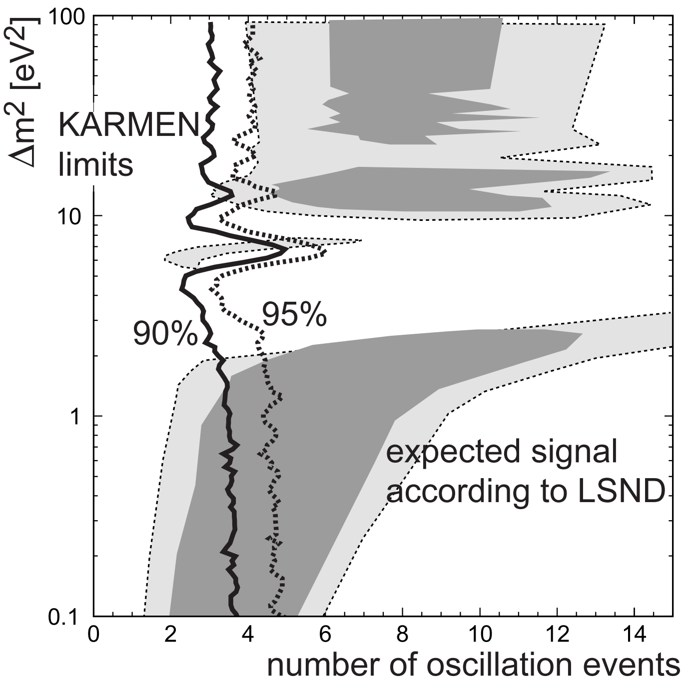

Figure 4: KARMEN exclusion limits at 90% CL and 99% CL in comparison with the range of expected oscillation events deduced from the LSND evidence [7)]. The darker (lighter) region corresponds to logarithmic likelihood values less than 2.3 (4.6) units below the global maximum.

limit of 3.8 and 3.1 oscillation events for $\Delta m^2 < 1\,\mathrm{eV}^2/\mathrm{c}^4$ and $\Delta m^2 > 20\,\mathrm{eV}^2/\mathrm{c}^4$, respectively, can be extracted at 90% CL based on a complete frequentist approach as suggested by [6)].

The limits at 90% CL and 99% CL can be compared with the number of oscillation events expected from the latest results of the LSND experiment [7]. In Figure 4, the calculated LSND signal strength within the KARMEN detector is shown. For large Δm^2, even at 99% CL, all of the favored LSND signal range can be excluded by KARMEN2. At lower values of Δm^2, a small fraction of the signal strength of LSND cannot be ruled out by KARMEN2. Note that at high Δm^2 the band of expected events and the exclusion curve are almost parallel. With decreasing values of Δm^2 the expected signal strength becomes smaller. This may be attributed, in part, to the larger source distance for the LSND experiment ($\langle d_{LSND}\rangle \approx 30\,$m compared to $\langle d_{KARMEN}\rangle \approx 17.7\,$m) but may also reflect a smaller signal strength: If the LSND data evaluation yields an oscillation probability $P(\bar{\nu}_\mu \rightarrow \bar{\nu}_e)$ which decreases with smaller values of Δm^2 –instead of remaining constant– this would have the same effect.

Assuming maximal mixing ($\sin^2(2\Theta) = 1$), 2442 ± 269 (e^+,n) sequences from oscillations with large Δm^2 were expected. Together with the limit of 3.1 events

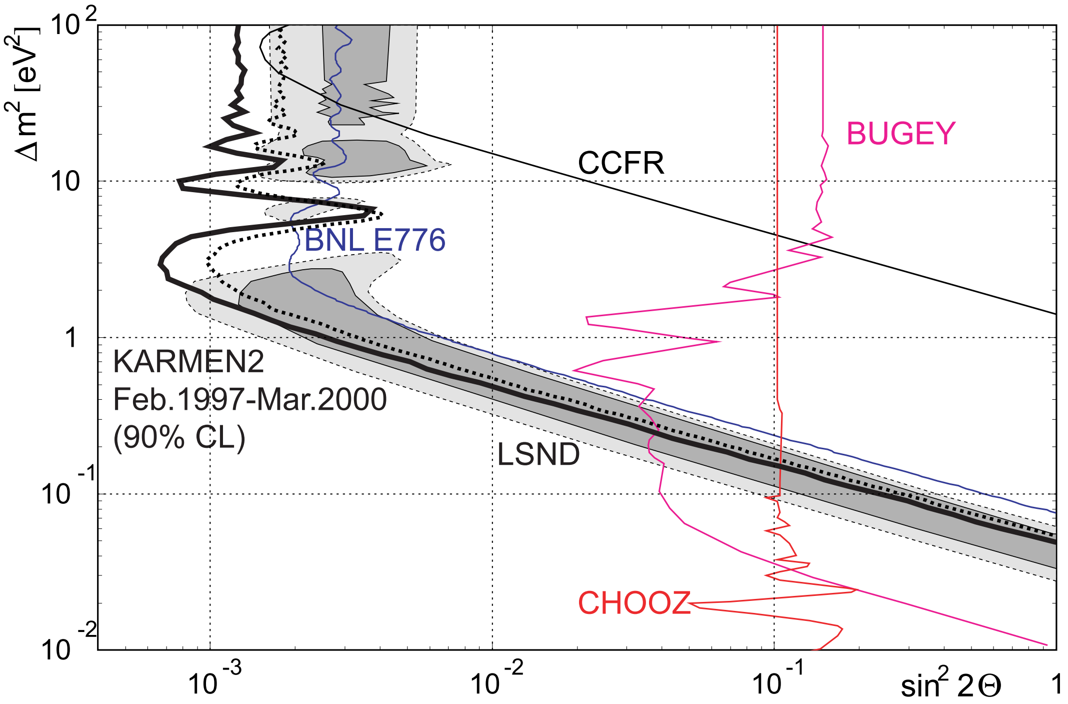

Figure 5: KARMEN2 exclusion limit and sensitivity (dashed line) at 90% CL compared to other experiments: BNL E776 [8], CCFR [9], BUGEY [10], CHOOZ [11] and the evidence for $\bar{\nu}_\mu \rightarrow \bar{\nu}_e$ oscillations reported by LSND [7].

deduced in the unified frequentist approach, this leads to an upper limit on the mixing amplitude of

$$\sin^2(2\Theta) < 1.3 \cdot 10^{-3} \qquad (90\%\,\mathrm{CL})$$

for $\Delta m^2 \geq 100\,\mathrm{eV}^2/\mathrm{c}^4$. The corrsponding exclusion curve in (Δm^2,$\sin^2(2\Theta)$) is given in Fig. 5. Also shown are limits from other experiments [8,9,10,11] as well as the favored regions from LSND based on a complete re-analysis of the entire 1993-98 data set [7]. Again, at high Δm^2, KARMEN excludes the region favored by LSND. At low Δm^2, KARMEN leaves some statistical space, but the reactor experiments at Bugey and Chooz add stringent limits from the $\bar{\nu}_e$ disappearance search. Any exclusion curve or favored region is a compactification of a complex statistical information, it reflects only a contour of the twodimensional likelihood functions which have nontrivial properties like multiple side maxima and non-parabolic shapes. Therefore, one needs a quantitative statistical analysis of both LSND and KARMEN based on the detailed event-by-event information as demonstrated in [12] for preliminary data sets to deduce correct statements of compatibility or disagreement in terms of frequentist confidence regions.

Taking the LSND region published first [13] which corresponds to a stronger $\bar{\nu}_\mu \rightarrow \bar{\nu}_e$ signal, there is a much stronger disagreement in the experiments' outcome: The actual 90% CL KARMEN2 limit excludes the complete parameter range favored by the 1993-95 LSND data.

One way of estimating the sensitivity of an experiment is to determine the average limit on the oscillation parameter simulating a large number of experimental outcomes with the actual level of background events, but no oscillation signal. These samples are subsequently analysed with the same maximum likelihood analysis used for the real data set. The actual KARMEN limit is slightly better than its sensitivity of $\sin^2(2\Theta) = 1.8 \cdot 10^{-3}$ for large Δm^2 and almost identical at lower Δm^2 (see dashed line in Fig. 5). Compared to the earlier results of KARMEN [5], this corresponds to an improvement of the sensitivity by a factor of ≈ 2.5.

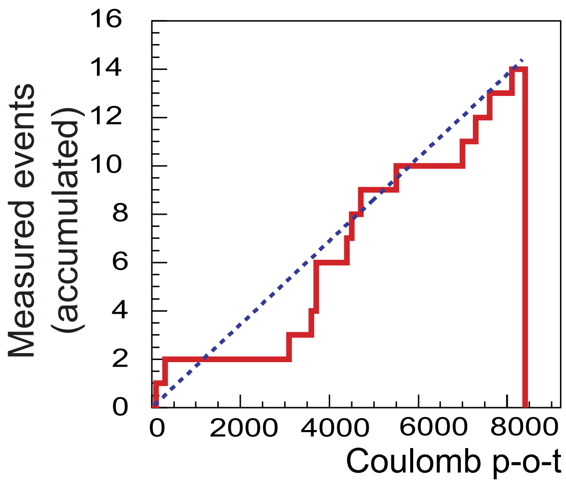

Figure 6: Accumulated oscillation candidates. The dashed line shows the corresponding expected total background.

Figure 6 reflects the number of accumulated oscillation candidate events as a function of the collected proton beam charge at ISIS. The analysis presented in this report is based on 7160 C beam charge. Meanwhile, data equivalent to 1200 C more of beam charge have been evaluated. 14 candidate events have been reduced with an expected background of 14.3 events (see dashed line in Fig. 6). The final oscillation analysis will comprise the whole data set with an accumulated neutrino flux corresponding to 9400 C of protons-on-target. The anticipated sensitivity will then reach $\sin^2(2\Theta) = 1.3 \cdot 10^{-3}$ for large Δm^2.

KARMEN has stopped data taking in April 2001, having seen no hint for neutrino oscillations so far. A new effort to cross-check the LSND parameter region is the upcoming BooNE experiment at Fermilab which is under construction. Its sensitivity is expected to improve the final KARMEN sensitivity by another factor of 2 [14] in the appearance mode $\nu_\mu \rightarrow \nu_e$ with different systematics than KARMEN and LSND.

3. References

1) KARMEN collaboration:
G. Drexlin, K. Eitel, T. Jannakos, M. Kleifges, J. Kleinfeller, C. Oehler, P. Plischke, J. Reichenbacher, M. Steidl, B. Zeitnitz: *Institut für Kernphysik, Forschungszentrum Karlsruhe, Institut für experimentelle Kernphysik, Universität Karlsruhe*
B.A. Bodmann, E. Finckh, J. Hößl, P. Jünger, W. Kretschmer: *Physikalisches Institut, Universität Erlangen-Nürnberg*
C. Eichner, R. Maschuw, C. Ruf: *Institut für Strahlen- und Kernphysik, Universität Bonn*
I.M. Blair, J.A. Edgington: *Physics Department, Queen Mary and Westfield College, London*
N.E. Booth: *Department of Physics, University of Oxford*
2) R.L. Burman *et al*, *Nucl. Instrum. Methods* A **368**, 416 (1996).
3) G. Drexlin *et al*, *Nucl. Instrum. Methods* A **289**, 490 (1990).
4) G. Drexlin *et al*, *Prog. Part. Nucl. Physics* **40**, 193 (1998).
5) K. Eitel and B. Zeitnitz, *Nucl. Phys.* B (proc. suppl.) **77**, 212 (1999).
6) G. Feldman and R. Cousins, *Phys. Rev.* D **57**, 3873 (1998)
7) I. Stancu, these proceedings; A. Aguilar *et al.*, *hep-ex/0104049*
8) L. Borodovsky *et al.*, *Phys. Rev. Lett.* **68**, 274 (1992).
9) A. Romosan *et al.*, *Phys. Rev. Lett.* **78**, 2912 (1997).
10) B. Achkar *et al*, *Nucl. Phys.* B **434**, 503 (1995).
11) M. Apollonio *et al*, *Phys. Lett.* B **348**, 19 (1995).
12) K. Eitel, *New J. Phys.* **2**, 1.1 (2000).
13) C. Athanassopoulos *et al*, *Phys. Rev.* C **54**, 2685 (1996).
14) A. Bazarko, *Nucl. Phys.* B (proc. suppl.) **91**, 210 (2001).